1124
3

Study of the Effect of Sensor Position on the Forced Response Characteristics of Rotors with Active Magnetic Bearings

by

Dharamendra Niranjan Rawal

Thesis submitted to the Faculty of the

Virginia Polytechnic Institute and State University

in partial fulfillment of the requirements for the degree of

Master of Science

in

Mechanical Engineering

APPROVED:

R. G. Kirk, Chairman

D. A. Elrod

L. D. Mitchell

August, 1990

Blacksburg, Virginia

LD
5655
V855
1990
R383
C.2

Study of the Effect of Sensor Position on the Forced Response Characteristics of Rotors with Active Magnetic Bearings

by

Dharamendra Niranjan Rawal

R. G. Kirk, Chairman

Mechanical Engineering

(ABSTRACT)

The need for better performance of turbomachinery with active magnetic bearings has necessitated a study of such systems for accurate prediction of their vibrational characteristics. This research presents a modification of existing transfer matrix methods for rotor analysis, to predict the response of rotor systems with active magnetic bearings. The position of the magnetic bearing sensors is taken into account and the effect of changing sensor position on the vibrational characteristics of rotor systems is studied. The modified algorithm is validated using a simpler modified Jeffcott model. The effect of changing from a rotating unbalance excitation to a constant excitation in a single plane is also studied. An eight-stage centrifugal compressor rotor is analyzed using the modified transfer matrix code. The results for a two-mass Jeffcott model are presented as plots of critical frequency vs. sensor position and amplitude at critical frequency vs. sensor position. Plots of amplitude vs. frequency and phase angle vs. frequency for different cases of sensor location are also presented. The results obtained by analyzing this two-mass model with the modified transfer matrix method have been compared with the results of the modified Jeffcott analysis for the purpose of verification. Also included are plots of amplitude vs. frequency and phase angle vs. frequency for the eight-stage centrifugal compressor rotor. These plots will demonstrate the significant influence that sensor location has on the critical frequencies and the amplitudes at the critical frequencies of the rotor system.

Acknowledgements

My thanks go to Dr. Kirk for giving me an opportunity to work on this interesting project and for guiding me throughout the course of it. I also thank John Keesee with whom it has been such a pleasure to work. His comments and suggestions have proved very useful. Dr. Mitchell and Dr. Elrod have given me their valuable time and expertise and I acknowledge their help and support. Finally I sincerely thank my parents for helping and supporting me throughout the duration of my study, and for always being there when I needed them.

Table of Contents

INTRODUCTION AND LITERATURE SEARCH 1

Previous Research 5

Research Objective 5

THE JEFFCOTT MODEL 7

The AMB Modification 8

Derivation of Modified Equations 12

Discussion of Plots 19

Results of the Modified Jeffcott Model 22

THE MODIFIED TRANSFER MATRIX METHOD 53

Modification for Sensor Non-Colocation 60

Algorithm for Modification Due to Sensor Non-Colocation 60

Discussion of the Convergence Process 65

Modification to Separate Gyroscopic Forces and Transverse Forces Acting at the Point Mass Stations 67

Obtaining the Solution with the Transfer Matrix Method 67

Comparison of the Results of the two-Mass Rotor System, for the Jeffcott Model and the Transfer Matrix Method 68
The Eight-Stage Centrifugal Compressor Rotor System Model 73
Discussion of the Plots 73
Results Obtained from the Eight-Stage Compressor Rotor System 77

CONCLUSIONS AND RECOMMENDATIONS **93**

BIBLIOGRAPHY **96**

Appendix A. DATA FOR THE TWO MASS JEFFCOTT MODEL IN SI UNITS **98**

Appendix B. DATA FOR THE TWO MASS JEFFCOTT MODEL IN ENGLISH UNITS **101**

Appendix C. DATA FOR EIGHT STAGE CENTRIFUGAL COMPRESSOR ROTOR IN SI UNITS **104**

Appendix D. DATA FOR EIGHT STAGE CENTRIFUGAL COMPRESSOR ROTOR IN ENGLISH UNITS **108**

Appendix E. MODIFIED JEFFCOTT ANALYSIS PROGRAM CODE **112**

Appendix F. GUIDE FOR RUNNING THE MODIFIED TRANSFER MATRIX PROGRAM **117**
GENERATION OF THE INPUT DATA FILE FOR PROGRAM FLXK 119
INTERPRETATION AND USE OF THE OUTPUT FILES 123
USING THE UTLPLT PROGRAM 124

Appendix G. ADDITIONAL PLOTS ILLUSTRATING SENSOR INFLUENCE ON VIBRATIONAL CHARACTERISTICS OF THE TWO-MASS MODEL 126

VITA 160

List of Illustrations

Figure 1. Picture of Active Magnetic Bearing (Courtesy of Magnetic Bearings, Inc., USA) . . 3

Figure 2. Active Magnetic Bearing Configuration (Zlotykamien, 1988) 4

Figure 3. Original Jeffcott Model 9

Figure 4. Geometry of Original Jeffcott Model 10

Figure 5. Single DOF Representation of the Jeffcott Model 11

Figure 6. The Modified Jeffcott Model 13

Figure 7. Geometry of the Modified Jeffcott Model 14

Figure 8. Reduced Two DOF Representation of the Modified Jeffcott Model 15

Figure 9. Freebody Diagram of the Modified Jeffcott Model 17

Figure 10. Mode Shapes for the Modified Jeffcott Model 18

Figure 11. Sensor Influence on Bearing Amplitude, Unbalance Excitation, M = 1, K = 2. . . . 26

Figure 12. Sensor Influence on First Critical Frequency, Unbalance Excitation, Journal Location, Amplification factor = 10 27

Figure 13. Sensor Influence on First Critical Frequency, Unbalance Excitation, Midspan Location, Amplification factor = 10 28

Figure 14. Sensor Influence on Third Critical Frequency, Unbalance Excitation, Journal Location, Amplification factor = 10 29

Figure 15. Sensor Influence on Third Critical Frequency, Unbalance Excitation, Midspan Location, Amplification factor = 10 30

Figure 16. Sensor Influence on First Critical Frequency, Unbalance Excitation, Journal Location, Amplification factor = 0.5 31

Figure 17. Sensor Influence on First Critical Frequency, Unbalance Excitation, Midspan Location, Amplification factor = 0.5 32

Figure 18. Sensor Influence on Journal Amplitude, Unbalance Excitation, First Critical Frequency, Amplification factor = 10 33

Figure 19. Sensor Influence on Midspan Amplitude, Unbalance Excitation, First Critical Frequency, Amplification factor = 10 34

Figure 20. Sensor Influence on Journal Amplitude, Unbalance Excitation, Third Critical Frequency, Amplification factor = 10 35

Figure 21. Sensor Influence on Midspan Amplitude, Unbalance Excitation, Third Critical Frequency, Amplification factor = 10 36

Figure 22. Sensor Influence on Journal Amplitude, Unbalance Excitation, First Critical Frequency, Amplification factor = 0.5 37

Figure 23. Sensor Influence on Midspan Amplitude, Unbalance Excitation, First Critical Frequency, Amplification factor = 0.5 38

Figure 24. Influence of Mass Ratio on Peak Amplitudes, Unbalance Excitation, Journal Location, Amplification factor = 0.5 39

Figure 25. Sensor Influence on First Critical Frequency, Planar Excitation, Journal Location, Amplification factor = 10 40

Figure 26. Sensor Influence on First Critical Frequency, Planar Excitation, Midspan Location, Amplification factor = 10 41

Figure 27. Sensor Influence on Third Critical Frequency, Planar Excitation, Journal Location, Amplification factor = 10 42

Figure 28. Sensor Influence on Third Critical Frequency, Planar Excitation, Midspan Location, Amplification factor = 10 43

Figure 29. Sensor Influence on First Critical Frequency, Planar Excitation, Journal Location, Amplification factor = 0.5 44

Figure 30. Sensor Influence on First Critical Frequency, Planar Excitation, Midspan Location, Amplification factor = 0.5 45

Figure 31. Sensor Influence on Journal Amplitude, Planar Excitation, First Critical Frequency, Amplification factor = 10 46

Figure 32. Sensor Influence on Midspan Amplitude, Planar Excitation, First Critical Frequency, Amplification factor = 10 47

Figure 33. Sensor Influence on Journal Amplitude, Planar Excitation, Third Critical Frequency, Amplification factor = 10 48

Figure 34. Sensor Influence on Midspan Amplitude, Planar Excitation, Third Critical Frequency, Amplification factor = 10 49

Figure 35. Sensor Influence on Journal Amplitude, Planar Excitation, First Critical Frequency, Amplification factor = 0.5 50

Figure 36. Sensor Influence on Midspan Amplitude, Planar Excitation, First Critical Frequency, Amplification factor = 0.5 51

Figure 37. Influence of Mass Ratio on Peak Amplitudes, Planar Excitation, Journal Location, Amplification factor = 0.5 52

Figure 38. Typical Rotor Section Element 55

Figure 39. Forces Acting on the Point Mass 56

Figure 40. Forces Acting on the Massless Elastic Shaft 58

Figure 41. Inboard Sensors 61

Figure 42. Outboard Sensors 62

Figure 43. Sensors on Either Side of the Bearings 63

Figure 44. The Eight-Stage Centrifugal Compressor Rotor System 74

Figure 45. Sensor Influence on Amplitude, Eight-Stage Compressor Rotor, Unbalance Excitation, First bearing 79

Figure 46. Sensor Influence on Amplitude, Eight-Stage Compressor Rotor, Unbalance Excitation, Midspan 80

Figure 47. Sensor Influence on Amplitude, Eight-Stage Compressor Rotor, Unbalance Excitation, Second bearing 81

Figure 48. Jeffcott Approximation of the Compressor Rotor, Unbalance Excitation, M = 1.326, K = 3.773, Inboard Sensors, Bearing 82

Figure 49. Jeffcott Approximation of the Compressor Rotor, Unbalance Excitation, M = 1.326, K = 3.773, Inboard Sensors, Midspan 83

Figure 50. Jeffcott Approximation of the Compressor Rotor, Unbalance Excitation, M = 1.326, K = 3.773, Outboard Sensors, Bearing 84

Figure 51. Sensor Influence on Mode Shapes, Eight-Stage Compressor Rotor, Unbalance Excitation, First Mode 85

Figure 52. Sensor Influence on Amplitude, Eight-Stage Compressor Rotor, Planar Excitation, First bearing 86

Figure 53. Sensor Influence on Amplitude, Eight-Stage Compressor Rotor, Planar Excitation, Midspan 87

Figure 54. Sensor Influence on Amplitude, Eight-Stage Compressor Rotor, Planar Excitation, Second bearing 88

Figure 55. Jeffcott Approximation of the Eight-Stage Compressor Rotor, Planar Excitation, M = 1.326, K = 3.773, Bearing 89

Figure 56. Jeffcott Approximation of the Eight-Stage Compressor Rotor, Planar Excitation, M = 1.326, K = 3.773, Midspan 90

Figure 57. Sensor Influence on Mode Shapes, Eight-Stage Compressor Rotor, Planar Excitation, First Mode 91

Figure 58. Influence of Sensor Location on Undamped Critical Speeds for First Four Modes, Eight-Stage Compressor Rotor (Keesee, 1989) 92

Figure 59. Sensor Influence on Bearing Amplitude, Unbalance Excitation, M = 1, K = 2 .. 128

Figure 60. Sensor Influence on Bearing Amplitude, Unbalance Excitation, M = 0.25, K = 2 129

Figure 61. Sensor Influence on Bearing Amplitude, Unbalance Excitation, M = 1, K = 0.5 . 130

Figure 62. Sensor Influence on Bearing Amplitude, Unbalance Excitation, M = 0.25, K = 0.5 131

Figure 63. Sensor Influence on Midspan Amplitude, Unbalance Excitation, M = 1, K = 2 .. 132

Figure 64. Sensor Influence on Midspan Amplitude, Unbalance Excitation, M = 0.25, K = 2 133

Figure 65. Sensor Influence on Midspan Amplitude, Unbalance Excitation, M = 1, K = 0.5 134

Figure 66. Sensor Influence on Midspan Amplitude, Unbalance Excitation, M = 0.25, K = 0.5 135

Figure 67. Sensor Influence on Bearing Phase, Unbalance Excitation, M = 1, K = 2 136

Figure 68. Sensor Influence on Bearing Phase, Unbalance Excitation, M = 0.25, K = 2 137

Figure 69. Sensor Influence on Bearing Phase, Unbalance Excitation, M = 1, K = 0.5 138

Figure 70. Sensor Influence on Bearing Phase, Unbalance Excitation, M = 0.25, K = 0.5 .. 139

Figure 71. Sensor Influence on Midspan Phase, Unbalance Excitation, M = 1, K = 2 140

Figure 72. Sensor Influence on Midspan Phase, Unbalance Excitation, M = 0.25, K = 2 ... 141

Figure 73. Sensor Influence on Midspan Phase, Unbalance Excitation, M = 1, K = 0.5 142

Figure 74. Sensor Influence on Midspan Phase, Unbalance Excitation, M = 0.25, K = 0.5 .. 143

Figure 75. Sensor Influence on Bearing Amplitude, Planar Excitation, M = 1, K = 2 144

Figure 76. Sensor Influence on Bearing Amplitude, Planar Excitation, M = 0.25, K = 2 ... 145

Figure 77. Sensor Influence on Bearing Amplitude, Planar Excitation, M = 1, K = 0.5 146

Figure 78. Sensor Influence on Bearing Amplitude, Planar Excitation, M = 0.25, K = 0.5 .. 147

Figure 79. Sensor Influence on Midspan Amplitude, Planar Excitation, M = 1, K = 2 148

Figure 80. Sensor Influence on Midspan Amplitude, Planar Excitation, M = 0.25, K = 2 .. 149

Figure 81. Sensor Influence on Midspan Amplitude, Planar Excitation, M = 1, K = 0.5 ... 150

Figure 82. Sensor Influence on Midspan Amplitude, Planar Excitation, M = 0.25, K = 0.5 . 151

Figure 83. Sensor Influence on Bearing Phase, Planar Excitation, M = 1, K = 2 152

Figure 84. Sensor Influence on Bearing Phase, Planar Excitation, M = 0.25, K = 2 153

Figure 85. Sensor Influence on Bearing Phase, Planar Excitation, M = 1, K = 0.5 154

Figure 86. Sensor Influence on Bearing Phase, Planar Excitation, M = 0.25, K = 0.5 155
Figure 87. Sensor Influence on Midspan Phase, Planar Excitation, M = 1, K = 2 156
Figure 88. Sensor Influence on Midspan Phase, Planar Excitation, M = 0.25, K = 2 157
Figure 89. Sensor Influence on Midspan Phase, Planar Excitation, M = 1, K = 0.5 158
Figure 90. Sensor Influence on Midspan Phase, Planar Excitation, M = 0.25, K = 0.5 159

List of Tables

Table 1. Data for Simple Two Mass Jeffcott Model AMB Rotor System 21

Table 2. Comparison of Different Convergence Schemes 66

Table 3. Results of the 2-Mass Rotor System, for the Jeffcott Model and the Transfer Matrix Model, Bearing Damping 0.263 Nsec/mm 69

Table 4. Results of the 2-Mass Rotor System, for the Jeffcott Model and the Transfer Matrix Model, Bearing Damping 0.263 Nsec/mm 70

Table 5. Results of the 2-Mass Rotor System, for the Jeffcott Model and the Transfer Matrix Model, Bearing Damping 0.263 Nsec/mm 71

Table 6. Results of the 2-Mass Rotor System, for the Jeffcott Model and the Transfer Matrix Model, Bearing Damping 0.263 Nsec/mm 72

Table 7. Data for Eight-Stage Centrifugal Rotor System Model 75

Nomenclature

a	eccentricity in 2 DOF Jeffcott model (mm)
a_x	eccentricity component in transfer matrix equation (mm)
a_y	eccentricity component in transfer matrix equation (mm)
C	damping (N-sec/mm)
E	modulus of elasticity (N/mm^2)
e	exponential constant = 2.7182818 (dim)
F_{xc}	externally applied planar excitation force in the transfer matrix equations (N)
F_{xs}	externally applied planar excitation force in the transfer matrix equations (N)
F_ϕ	constant excitation force in Jeffcott model (N)
I	moment of inertia of massless shaft (mm^4)
I_p	polar moment of inertia (mm^4)
I_t	transverse moment of inertia (mm^4)
i	complex constant (dim)
K	stiffness ratio, k_1/k_2 (dim)
K	stiffness in transfer matrix equations (N/mm)
k_1	AMB stiffness (N/mm)
k_2	shaft stiffness (N/mm)

L	length of shaft in 2 DOF Jeffcott model (mm)
l	length of massless shafts in transfer matrix equations (mm)
M	mass ratio, m_1/m_2 (dim)
M_1	effective journal mass in Jeffcott model (Kg)
M_2	mid-span mass in Jeffcott model (Kg)
M_{xc}	moment component in transfer matrix equation (N-mm^2)
M_{xs}	moment component in transfer matrix equation (N-mm^2)
m_i	point masses in transfer matrix equations (Kg)
R_i	complex solution of the Jeffcott model
r_i	whirl deflection in Jeffcott model
r_s	whirl deflection at sensor location in Jeffcott model
s	frequency of shaft rotation (rad/sec)
t	time (sec)
V_{xc}	shear component in transfer matrix equation (N)
V_{xs}	shear component in transfer matrix equation (N)
x_i	x component of the whirl deflection in the Jeffcott model (mm)
xc	deflection component in transfer matrix equations (mm)
xs	deflection component in transfer matrix equations (mm)
y_i	y component of the whirl deflection in the Jeffcott model (mm)
z	axial distance between sensor location and bearing sensor (mm)
α	ratio of the distance between bearing centerline and sensor to half-span of the rotor (dim)
θ_{xc}	slope component in the transfer matrix equation (rad)
θ_{xs}	slope component in the transfer matrix equation (rad)
ω	frequency of shaft excitation (rad/sec)

Chapter 1

INTRODUCTION AND LITERATURE SEARCH

The use of active magnetic bearings in turbomachinery is a comparatively new development but one which has shown great promise for better control of rotating equipment. The idea behind these bearings is not new however. The use of magnetic attraction to levitate the rotor shaft free of the bearing has been tried before, but because the system is inherently unstable (Hustak, 1985) unless a real-time control system is used, these attempts were not successful. The first actively controlled bearing was developed in the 1950's (Keesee, 1989). Since then the use of active magnetic bearings has gained widespread acceptance particularly in North America and Canada. Hendrickson et al (1987) give some examples of the varied uses to which active magnetic bearings have been applied. Kirk (1988) lists a number of turbomachinery installations where active magnetic bearings have been used.

The principle of how active magnetic bearings work is very simple. A magnet will attract any ferromagnetic material. Thus, the rotor shaft is wound with ferromagnetic lamination near the journal location. The stator is made up of slotted lamination stack and has coils wound around the

slots. When an electric current is supplied to the coils of lamination in the stator, the lamination acts as an electromagnet and attracts the ferromagnetic material on the rotor shaft. One such electromagnet is located in each of the four quadrants inclined at 45°. The attraction of each of these four electromagnets is varied by a control system to levitate the rotor shaft and keep it levitated while it is rotating. In order to enable the control system to decide the amount of attraction to be applied to the rotor shaft through each electromagnet, sensors are placed at some distance from the stator along the axis of the rotor shaft. These sensors sense the location of the shaft. The configuration is illustrated in Figs. 1 and 2.

Magnetic bearings possess a number of advantages compared to conventional bearings. They give an almost unlimited control over rotor vibrational characteristics due to adjustable stiffness and damping. Automatic balancing is possible by allowing the rotor to spin on its inertial axis. This leads to decreased vibrations and noise. Active magnetic bearings do not require lubrication, and since they are non-contact bearings, they eliminate the possibility of wear and tear of the stator and rotor surfaces. Hendrickson et al (1987) demonstrates the tolerance of magnetic bearings to a wide range of temperatures and also their insensitivity to hostile environments. Zlotykamien (1988) gives a good description of the various advantages of active magnetic bearings.

One of the main disadvantages of active magnetic bearings is the relatively high costs involved due to the presence of a complex control system. Since magnetic bearings require electricity to generate the magnetic field that keeps the rotor levitated, the possibility of power failure has to be taken into account and conventional backup bearings have to be provided. The weight of the rotor shaft has to be within the limits of the carrying capacity of magnetic bearings. Being a comparatively new development, the vibrational behaviour of rotor systems with magnetic bearings needs furthur study specially with respect to their stability characteristics.

Figure 1. Picture of Active Magnetic Bearing (Courtesy of Magnetic Bearings, Inc., USA)

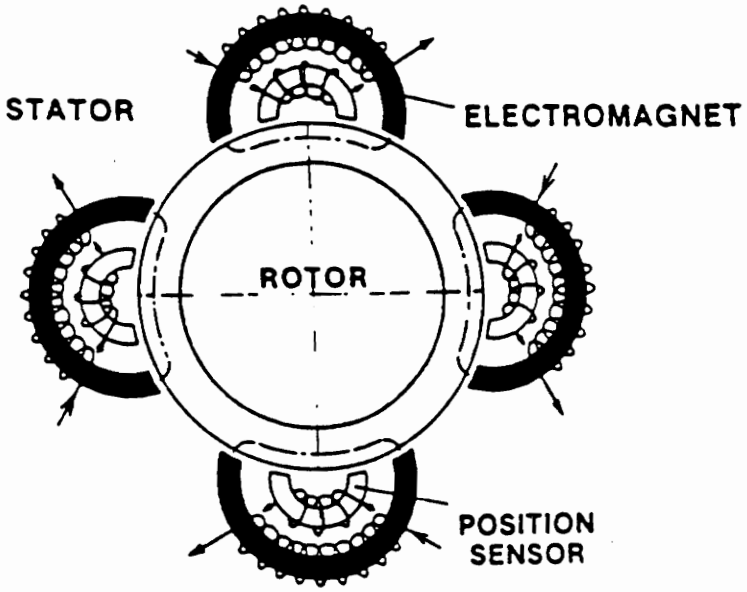

Figure 2. Active Magnetic Bearing Configuration (Zlotykamien, 1988)

Previous Research

Most of the research in active magnetic bearings has been in the control systems used. Schweitzer (1985) shows a method for controlling an elastic rotor so that it can be represented by a low-order model amenable to control techniques. Williams, Keith, and Allaire (1990) have developed theoretical relationships to relate the characteristics of a controller transfer function to the stiffness and damping properties of an active magnetic bearing. Burrows and Sahinkaya (1988) evaluate various strategies for applying a magnetic bearing to control the synchronous vibration of a flexible rotor. Kirk et al (1988) present the results of shop tests on a high-speed eight-stage centrifugal compressor supported by active magnetic bearings along with some design recommendations. Keesee (1989) examines the effects of sensor position on the critical frequencies of rotors with active magnetic bearing.

Research Objective

The sensors are not located at the place where the attraction forces are applied on the rotor shaft but at some distance away along the axis of the shaft. Due to this "non-colocation" of the sensors from the bearing position, the deflection sensed by the sensors is not the same as the actual deflection at the bearing but differs from it by some magnitude and phase, dictated by the mode shape of the rotor shaft. Because of this, the stiffness and damping forces of the active magnetic bearing depend not on the deflection at the bearing location, but on the deflection at the sensor location. For such cases, the vibrational characteristics of the rotor system is different from that obtained using conventional analysis programs. The objective of this research is to take into account the effect of sensor non-colocation on the vibrational characteristics of rotors with active magnetic bearings.

This research is an extension of the work done by Keesee (1989) and involves the modification of an existing transfer matrix code to account for sensor non-colocation. Sensor non-colocation effects on forced response amplitudes and phase angles are studied. The other objective of this research is to compare the vibrational characteristics of rotor systems, when they are subject to unbalance excitation with circular synchronous shaft rotation and excitation in one plane with no shaft rotation or whirling. The effect of changing the mass at the bearing locations with respect to the mass at midspan is studied. The effect of changing the stiffness of the bearings with respect to the stiffness of the shaft is studied. The effect of changing the amount of damping in the system is also studied.

Two models of rotor systems are used for this study. One is a simple two-mass Jeffcott model. The other is an eight-stage centrifugal compressor rotor model. The modification of the transfer matrix program is validated by comparing its results for the two-mass model with the results obtained from a simple program written to specifically analyze the two-mass model. Chapter 2 gives the theory of the Jeffcott model as well as the modification made to account for sensor non-colocation. It also gives the results obtained from the two-mass Jeffcott model. Chapter 3 details the theory of transfer matrices and the different modifications necessary to account for sensor non-colocation and excitation forces. The results of the typical eight-stage centrifugal rotor system are also illustrated in Chapter 3. These results provide the validation of the modifications made in the transfer matrix code. Chapter 4 gives the recommendations and conclusions of this research.The Appendix contains the Jeffcott model code, the data for the two-mass model and the eight-stage compressor rotor system model, guidelines for the use of the AMB (Active Magnetic Bearing) modified transfer matrix code and additional plots illustrating the effect of a change in sensor position on the vibrational characteristics of a two-mass rotor system.

Chapter 2

THE JEFFCOTT MODEL

Jeffcott (1919) has analyzed a simple rotor model composed of a long thin massless elastic shaft with a given stiffness and a central disk mass with a given unbalance. Since the unbalance force rotates at shaft speed, the frequency of whirl will be the same as the frequency of shaft rotation. Jeffcott assumes that the bearings are radially rigid. Thus, the system reduces to a single-degree-of-freedom vibrations problem as shown in Figs. 3-5.

The equations of motion for the system shown in Fig. 3 and Fig. 4 are as follows

$$M\frac{d^2}{dt^2}(x + a\cos\omega t) + C\frac{dx}{dt} + Kx = 0 \qquad [2.1]$$

$$M\frac{d^2}{dt^2}(y + a\sin\omega t) + C\frac{dy}{dt} + Ky = 0 \qquad [2.2]$$

These equations can be simplified and rewritten as follows

$$M\ddot{x} + C\dot{x} + Kx = M\omega^2 a\cos\omega t \qquad [2.3]$$

$$M\ddot{y} + C\dot{y} + Ky = M\omega^2 a\sin\omega t \qquad [2.4]$$

Henceforward, the complex variable $r = x + iy$ will be used to indicate the whirl radius in the Jeffcott model, and all the equations will be stated in terms of r. Equations 2.3 and 2.4 can be combined and written as a single equation by using complex algebra as follows

$$M\ddot{r} + C\dot{r} + Kr = M\omega^2 r \qquad [2.5]$$

The AMB Modification

To modify the Jeffcott model for active magnetic bearings, four additional factors are assumed.

- First, the stiffness and damping of the magnetic bearing are considered. This is because the forces due to bearing stiffness and damping depend on the deflection of shaft sensed by the active magnetic bearing sensor, and thus, are subject to change as the sensor position changes. A change in the excitation frequency will also change the shaft deflection sensed by the sensor and and consequently change the bearing stiffness and damping forces.

- Second, the presence of journal masses at the bearing locations is assumed. Thus, a central disk mass at midspan and the two journal masses at the bearings are considered in the formulation of the equations of motion.

- A harmonic excitation force in one plane F_ϕ that can be applied at the bearing locations is considered. This is so that a magnetic bearing rig can be tested without rotating the rotor shaft. Instead, the journal masses are excited at a particular frequency and the vibrational characteristics of the rig are examined. Unlike an unbalance force where the amplitude of the force changes with the rotor spinning speed, the amplitude of the planar harmonic excitation force remains constant irrespective of the rotor spinning speed and hence this force can also be termed as a constant magnitude excitation force.

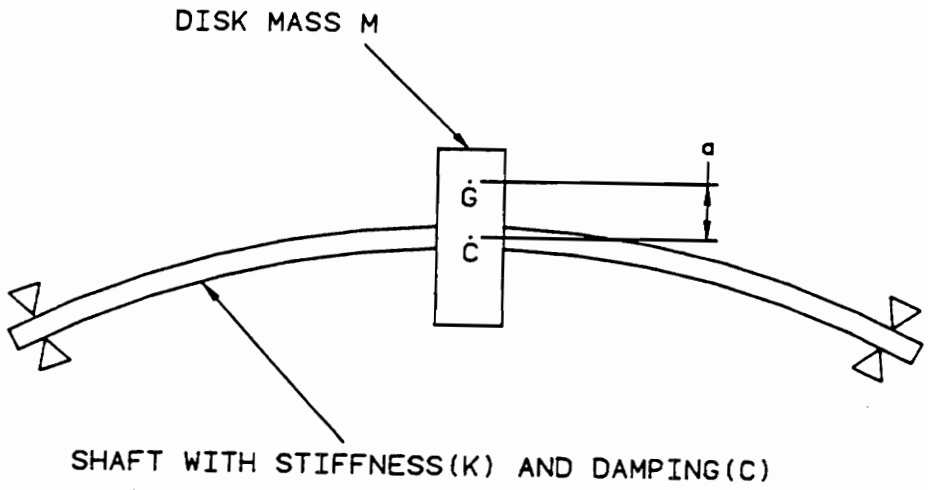

Figure 3. Original Jeffcott Model

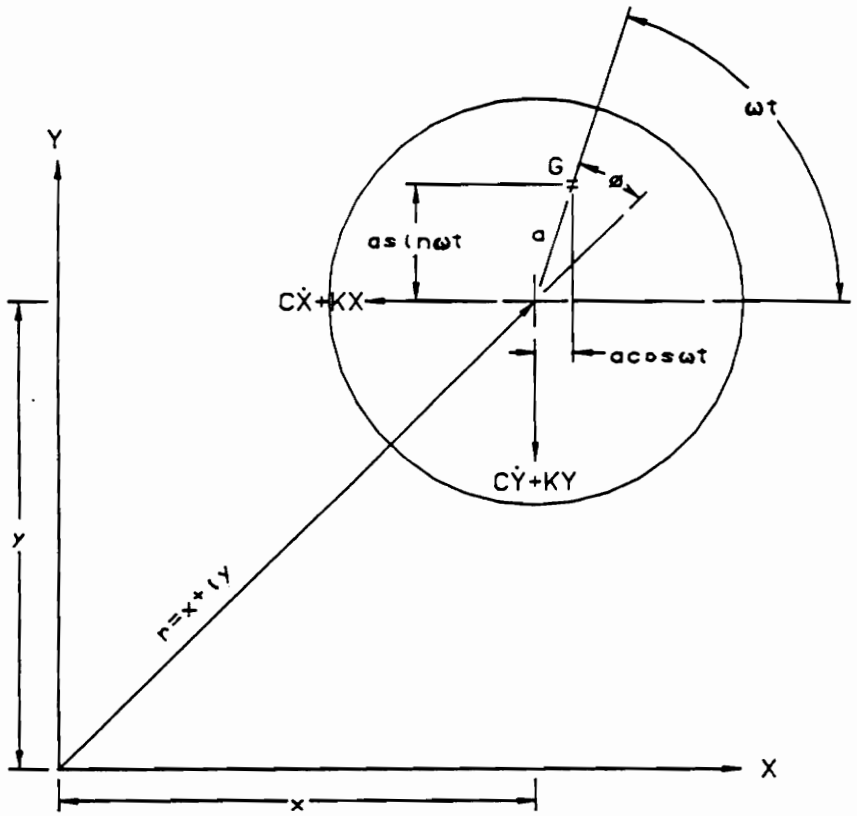

Figure 4. Geometry of Original Jeffcott Model

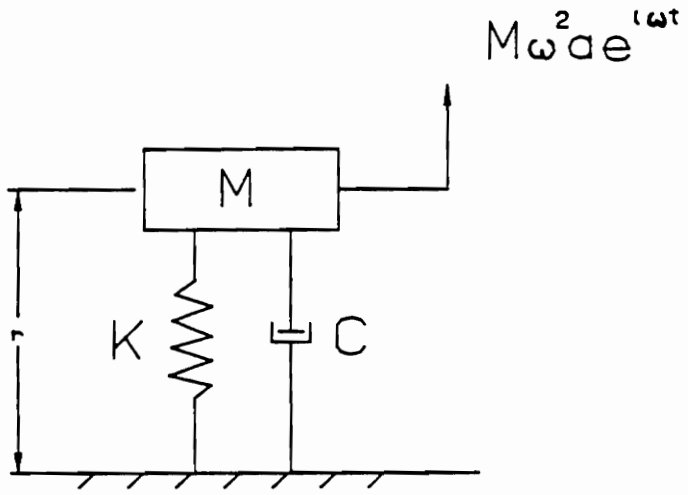

Figure 5. Single DOF Representation of the Jeffcott Model

- Lastly, consideration is given to the sensors that detect the deflection of the shaft at some distance from the bearings. This deflection is then used to modify the stiffness and damping characteristics of the active magnetic bearings.

The bearing pedestal is assumed to be rigid. The entire configuration after modification is illustrated in Figs. 6-8.

Since the unbalance force and the planar harmonic excitation force are applied symmetrically along the longitudinal axis of the rotor, only the first and third modes are observed. The second mode cannot be observed in the reduced two-mass model.

Derivation of Modified Equations

To formulate the equations of motion, consider the freebody diagram shown in Fig. 9.
Note that the forces on the mass M_1 depend on the deflection and velocity at the sensor location. To express the deflection at the sensor location (r_s) as a function of the deflection at the disk (r_2) and at the bearing (r_1), it is assumed that the first and third modes of vibration are half-sine curves. These modes are illustrated in Fig. 10. Thus

$$r_s = r_1 + (r_2 - r_1)\sin(\frac{\pi z}{L}) \qquad [2.6]$$

so that when $z = 0 \quad r_s = r_1$ and

when $z = L/2 \quad r_s = r_2$

The two equations of motion will be

$$M_2\ddot{r}_2 = M_2\omega^2 a e^{i\omega t} - C_2(\dot{r}_2 - \dot{r}_1) - K_2(r_2 - r_1) \qquad [2.7]$$

$$M_1\ddot{r}_1 = F_\phi e^{i\omega t} + C_2(\dot{r}_2 - \dot{r}_1) + K_2(r_2 - r_1) - C_1\dot{r}_s - K_1 r_s \qquad [2.8]$$